# Inclusive Production of $\pi^{\pm}$ in the Backward Direction from Complex Nuclear Targets

K. Abe, J. Alspector, R. Bomberowitz, K. J. Cohen
W. C. Harrison, B. Maglich, B. Robinson and F. Sannes

Rutgers University

New Brunswick, New Jersey   08903

April 1973

Proposal for Experiment at NAL

Inclusive Production of $\pi^{\pm}$ in the Backward Direction

from Complex Nuclear Targets

K. Abe, J. Alspector, R. Bomberowitz, K. J. Cohen,

W. C. Harrison, B. Maglich, B. Robinson and F. Sannes

Rutgers University

New Brunswick, New Jersey 08903

(201) 932-2531

April, 1973

## Introduction

We propose to measure simultaneously the inclusive cross sections for $\pi^+$ and $\pi^-$ production from complex nuclei in the backward direction. We propose to use a tagged positive beam and simultaneously measure

$$\pi^+ A \to \pi^\pm X \qquad (1)$$

$$p\,A \to \pi^\pm X \qquad (2)$$

The identity of the incident particle would be tagged with Cerenkov counters and we would differentiate $\pi^+$ from $\pi^-$ in the final state. We would determine $p_\perp$ and x (Feynman variable) for the produced particles by measuring $p_3$ and $\theta_3$ and cover a large range in each of these variables. We would study both the energy dependence (e.g., at 50, 100, and 200 GeV/c) and the A dependence (C, Al, Sn, and Pb) of reactions (1) and (2). As a by-product, events with either p or $\bar{p}$ in the final state would also be detected and stored.

## Motivation

The primary purpose of this experiment is to determine the contributions of two extreme categories of models to multi-particle production. The two categories of theoretical models are:

I.   CPP (Coherent Production Processes).

This category includes models such as diffraction excitation[1], nova model[2], one- or two-fireball models[3], and the particle fragmentation model[4]. These models assume that multi-particle production is a two-step process. In the first step, one or two systems are produced and these subsequently decay, with lifetimes long compared to the collision time, into the final multiparticle states.

## II.  IPP (Incoherent Production Processes)

This category includes the multiperipheral model[5] and its multi-Regge generalizations[6], and the bremsstrahlung analogy[7]. The essential characteristic of these models is that the final, multiparticle state is directly produced from the colliding particles in a single step.

The important point is that the models in both categories have been constructed to agree with existing data. To the best of our knowledge (see Table 1) there are no crucial experimental tests which would  decide which     class of multiparticle production is closer to reality .

Recently, several authors[8,9,10] have suggested using complex nuclear targets as "laboratories" in inclusive reactions to provide a sensitive method for making a distinction between IPP and CPP. The basic reasoning behind this suggestion is straightforward although in practice the calculations become complicated. That such calculations can, in principle, be carried out is not unreasonable because we know the elementary interactions from other experiments and we know the nature and distribution of the constituent nucleons. In addition, the Glauber model seems to give a good description of the multiple-scattering of high energy particles in nuclei.

The essential difference between IPP and CPP in a complex nucleus is illustrated in Figures  1 and 2.

I.  CPP. Because the fireball is assumed to decay after passing through the nucleus, the problem becomes one of mean-free-paths. Contributions to the final state can be divided into two parts:

1) Contributions from the fragmented projectile.

2) Contributions from target fragmentation.

These two contributions can be differentiated by considering the number distribution $\frac{dn}{dx}$ as a function of the Feynman variable $x = \frac{2q^*_{11}}{\sqrt{s}}$ ($q^*_{11}$ is the longitudinal momentum of the observed particle in the c.m., and s is the square of the total c.m. energy). For $-\frac{1}{A} \le x < o$ we are in the region of target fragmentation[11] while for $o < x < 1$ we are in the region of projectile fragmentation. Consider the number distribution as a function of the A of the target and of the incident energy E:

i) A dependence. For target fragmentation (negative x) the number of produced particles should go like the number of collisions experienced by the fireball in the nucleus and this is proportional to $A^{1/3}$. Predictions for positive x are not so clear because the evolution of the fireball with successive scatterings is not understood. (To first order, one might assume the contribution to be A-independent.)

ii) Energy dependence. Once one is in the region for scaling for inclusive production from nucleons, CPP should be energy independent. I.e., scaling should be observed for inclusive production from nuclei.

II. IPP. The interaction for IPP is shown in Figure 2. This is more complex than CPP. It is assumed that particles belonging to the final state of a hadronic reaction are created incoherently so that as they propagate through the nucleus they can independently participate

in further particle production. In this manner an intranuclear cascade is produced (similar in some respects to the formation of an electromagnetic shower). The reaction $\pi N \to \pi X$ can cascade many possible ways in the nucleus to contribute to the process $\pi A \to \pi X$. Fig. 2 is only one such diagram. In this diagram, the incident particle penetrates into the nucleus to point $z_1$ where an inelastic collision takes place. Let $\phi$ represent the number of particles created in the collision. Then each of these $\phi$ particles will proceed through the nucleus and some of them will undergo inelastic collisions themselves (for example, at $z_2$, $z_3$ and $z_4$ in the figure) creating still more particles. Between inelastic collisions, each particle can undergo any number of elastic scatterings from nucleons. It is clear that, if we wish to calculate the number distribution of the outgoing particles, we must perform a properly weighted sum over the distribution for any diagram which leads to particles of the type we wish to measure coming out of the nucleus.

i) A dependence. At AGS energies, the number distribution for IPP should be A independent for $A \gtrsim 10$. This is because the cascade will be fully developed after the first few layers of nucleons. As $s \to \infty$ the number distribution should go like A. At NAL we should see a different A dependence at each energy.

ii) <u>Energy dependence</u>. For IPP, there will be an energy
dependence for the number distribution. For each
interaction in the cascade, the produced particles
will have an energy distribution which depends on the
incident energy in the collision. And this energy
distribution affects the interactions in future
generations. The exact energy dependence is not simple
and is somewhat model dependent. The important point
is here there will be <u>no scaling</u> for production from nuclei

So each category of multiparticle production models has
a clear signature in dependence on incident energy and dependence on
the A of the nuclear target. Two methods have been suggested to
use these properties to distinguish CPP and IPP:

1) <u>Trefil and Fishbane</u>[8] point out that a measurement of
the inclusive cross section $d\sigma/dx$ in the backward direction would
be a very effective method to differentiate CPP and IPP. (The
inclusive cross section and the number distribution are simply
related by $\frac{dn}{dx} = \frac{1}{\sigma_{tot}} \frac{d\sigma}{dx}$ .)

2) <u>Dar and Vary</u>[9] suggest measuring the average multiplicity
as a function of A and E.

Method 2) however, requires more assumptions than 1) and
is not so sensitive in detecting an A dependence for CPP because
contributions to $<n>$ for $x > 0$ are probably A independent. In
addition, method 1) gives more information with our proposed exper-
iment than 2). We will measure the inclusive cross section in the
backward direction as a function of x and $p_\perp$ whereas the $<n>$ =

$\frac{1}{\sigma_{tot}} \int \frac{d\sigma}{dx}$ integrates over most of this information. A knowledge of the x distribution and the $P_{\perp}$ distribution will allow a check on factorization.* We will also measure the $\pi^+/\pi^-$ ratio which could be of interest in some models of particle production. A measurement of <n> vs A, E has been proposed (NAL proposal #178) by Busza et al. No one has yet systematically measured the inclusive cross section in the backward direction from complex nuclei.

Another method of distinguishing IPP and CPP is to look at correlations in two particle inclusive reactions on protons. Investigation along these lines is currently underway at CERN.[12]

Besides investigating models of multiparticle production, the study of inclusive cross section on complex nuclei is interesting for other reasons:

1) Ultra-high-energy data is obtained presently only from cosmic ray interactions in nuclear emulsions. From these data one wants to extract information about the more fundamental nuclear interaction and strong-interaction dynamics. Theoretically this is the inverse of the problem discussed above.

2) In order to study the cosmic rays themselves, we must know how they interact with atmospheric and emulsion nuclei and how cascade showers develop.

3) Secondary beams are produced by bombarding nuclear targets. An understanding of these processes could be useful.

*See footnote, page 7.

4) The understanding gained from studying the composite system of a nucleus might be applied to hadronic processes by assuming hadrons are composite systems whose constituents are partons.

## Description of Experimental Goals

As discussed above, the most sensitive method yet suggested to differentiate CPP and IPP in multiparticle production is to study the A dependence and/or the energy dependence of inclusive cross sections in the target fragmentation region using complex nuclear targets.

To efficiently collect a large amount of information we propose to simultaneously measure $\pi^+$ and $\pi^-$ in the final state and to cover a large range in $p_\perp$ and negative x. This will allow us to study both the x distribution and the $p_\perp$ distribution (and thus check factorization$^*$) and the $\pi^+/\pi^-$ ratio. If all data for a given incident energy and a given target can be taken at a single spectrometer setting, systematic errors will be minimized and data acquisition maximized.

Choice of targets was motivated by a necessity to distinguish between the predictions of IPP and the predictions of CPP. We will measure the inclusive cross section which is related to the number distribution dn/dx by:

$^*$i.e., is the cross section of the form $f(x)g(p_\perp)$ ?

$\frac{d\sigma}{dx} = \sigma_{TOT} \frac{dn}{dx}$ . Since $\sigma_{TOT} \propto A^{2/3}$, our measured inclusive cross

sections should go like $A^{2/3} \xrightarrow[s\to\infty]{} A^{5/3}$ for IPP and like A for

CPP.

TABLE 2

| Element | A | $A^{2/3}$ |
|---------|-----|-----------|
| Carbon | 12 | 5.2 |
| Aluminum | 27 | 9.0 |
| Tin | 119 | 24.0 |
| Lead | 208 | 35.0 |

We would simultaneously measure the processes

$$\pi^+ A \to \pi^\pm X$$

$$p A \to \pi^\pm X$$

and we would take equal amounts of data at three energies (e.g.,
50, 100, and 200 GeV/c). As a by-product we will also store
events (see below) with p or $\bar{p}$ in the final state.

## Design Considerations

A) We want to measure with a fixed configuration inclusive cross sections over a large range of negative x and over a large range of $p_\perp$ with targets ranging from carbon to lead. A look at the kinematics graphs (Fig. 3) shows that this requires a spectrometer covering lab angles from 90° to 150° and accepting momenta from 100 MeV/c to 600 MeV/c. Since both $\pi^+$ and $\pi^-$ are to be measured simultaneously the spectrometer should be symmetric about 120°.

B) We are interested mainly in the general shape and height of the x distribution, not in detailed structure. An angular resulution of ±1° and a momentum resolution of ±50 MeV/c at the high end are adequate. Thus a rough trajectory determination using only counters is indicated. This also keeps the experiment simple. A position determination of ∿1/2" gives the necessary resolution.

C) We want to use available equipment. We have a sixty counter hodoscope from a previous experiment[13] that is ideal and a magnet similar to the one described below would have the proper parameters.

## Description of Spectrometer

The spectrometer consists of a magnet with hodoscopes in front and behind as shown in figure 4. The "point" target and front hodoscope determine the trajectory entering the magnet. The rear hodoscope determines the exit trajectory and thus the angle of bend and momentum.

The front hodoscope consists of 60 counters each 1/4" thick, 4" high, 1/2" wide. The rear hodoscope consists of 128

counters 1/4" thick, 10" high and 9/16" wide. They are positioned as far away from the target as their lengths (30" and 72" respectively) and about 1' away from the magnet on either side. The magnet should have a height of 10", a 6' wide gap and $\int Bdl \simeq 4$ Kilogauss-meters. It should have shield plates on either side to keep the field uniform and reduce its effect on the hodoscope photomultipliers.

The target will be a slab of material $\leq$ 1/2" thick and at an angle of about 20$^O$ with respect to the beam. Its height and width will be large compared to beam size so that all beam particles detected by a set of trigger counters will pass through it for normalization purposes. The beam spot should be $\lesssim$ 1" wide at the target for good angular resolution. Behind the rear hodoscope will be a 12" by 78" counter to determine the time of flight (TOF) of the particle from the target. It will have a phototube on each side to correct for time differences due to scintillation light travel time. The counter in the rear hodoscope which fires gives a further check on the TOF. We should have a 1 ns TOF resolution. Over the momentum range of interest (100 to 600 MeV/c), protons will be at least 5 nanoseconds slower in reaching this counter than pions, making πp separation easy.

## Electronics

Our event trigger will consist of an incident beam particle detected by a set of beam counters in coincidence with our TOF counter. When an event is detected, all hodoscope counters are strobed and a 24 bit word is encoded by a set of logical integrated circuits.

The breakdown of the 24 bit word is as follows:

  6 bits - counter number in front hodoscope (1→60)

  7 bits - counter number in rear hodoscope (1→128)

  6 bits - time of flight of particle

  4 bits - pulse height in TOF counter

  1 bit  - flag if more than one counter in each

            hodoscope fires.

If both π's and p's are in our incident beam one of these bits would tag which particle is incident.

This 24 bit word is stored in the memory of a 4096 channel multi-channel analyzer. After the memory fills (4096 events), it is dumped onto magnetic tape. Total time to encode an event is about 10 microseconds so that dead time is negligible. If more than one counter fires, we can use the flag bit to store more than one word. It would then indicate continuation. A data collection system similar to this is now in operation in a Rutgers experiment (#67) at NAL.

## Monte-Carlo Studies

To optimize and further study the parameters of our spectrometer we have developed a Monte Carlo simulation. This program includes both $\frac{dE}{dx}$ and multiple scattering in our target and counters.

We used these studies to optimize the angle of the target with respect to the beam line, $\phi_T$, and the target thickness, t, and to calculate the resulting resolutions within our acceptance.

1) $\underline{\phi_T}$. Here a compromise is necessary between two effects. For optimization of the intrinsic resolution of the spectrometer

we want the beam spot seen by the hodoscopes to be minimized. On the other hand, to reduce the effects of dE/dx and multiple scattering, the target should be rotated to reduce the path length of particles leaving the target. The results for a lead target and 175 GeV/c incident protons are shown in figure 5 for two ranges of final momenta and 3 ranges of final angle. The optimum value for $\phi$ is $\sim 20^\circ$ for the best resolution in x and in $p_\perp$. Similar results were obtained for carbon and aluminum.

2) <u>Target thickness</u>. One wishes to optimize the counting rate without destroying resolution due to dE/dx effects and multiple Coulomb scattering. Since these effects are adding in quadrature with the intrinsic resolution of the spectrometer, the resolution remains flat as a function of target thickness until the two contributions became comparable. This behavior is shown for aluminum in figure 5 - again we consider the resolution in x and the resolution in $p_\perp$ for 175 GeV/c incident protons. The optimal value for aluminum is 1/2". The result obtained for carbon was also 1/2", 3/8" for tin, and for lead we found that resolution quickly deteriorated for t> 1/4".

3) <u>Resolution</u>. Figure 6 shows the x and $p_\perp$ resolution of our apparatus at various points in our acceptance for the optimum parameters found above. The length of the errors correspond to one standard deviation. We show results for carbon and lead.

Other problems are the effects of multiple interactions and $\pi^\circ$ conversion in the target. These effects can be corrected for by taking data at several target thicknesses and extrapolating the results to t=0. We would run at the maximum thicknesses found above ($t_o$) as well as $t_o/2$ and $t_o/4$.

## Counting Rates

Lower limits on expected counting rates were determined by integrating inclusive cross sections for $\pi^+ p \rightarrow \pi^\pm X$ and $pp \rightarrow \pi^\pm X$ over the acceptance of our apparatus. Rates from complex nuclear targets will be $\geq A^{2/3}$ times the results calculated using data from proton targets.

For example, consider $\pi^+ Al \rightarrow \pi^+ X$ with a 1/2" Al target

$$\Delta\sigma = 0.0258 \text{ mb} \quad \text{for } \pi^+ p \rightarrow \pi^+ X$$

$$N_t = 7.65 \times 10^{22} \text{ nuclei for 1/2" Al}$$

$$N_i = 2.5 \times 10^6 \ \pi^+ / \text{ pulse}$$

So, Rate $\geq A^{2/3} \Delta\sigma N_i N_t = 44.08$ events/pulse or, assuming $\sim 1$ pulse/5 sec, $\sim 760000$ events/day.

Considering all reactions, we find for our acceptance the following ratios for $\Delta\sigma$:

$$\pi^+ p \rightarrow \pi^+ X \ / \ \pi^+ p \rightarrow \pi^- X \ / \ pp \rightarrow \pi^+ X \ / \ pp \rightarrow \pi^- X$$

$$= \quad 1.0 \quad / \quad 0.212 \quad / \quad 1.55 \quad / \quad 0.606$$

Using these results, we calculated the lower limits for the rates/pulse given in Table 3 in the same manner as above. Also shown (in parentheses) are the corresponding rates/day. As above, we assumed $2.5 \times 10^6$ incident particles/pulse. Table 4 shows the distribution as a function of x and $p_\perp$ for 1/2" Al for one day. The rates for the other targets are approximately the same.

We note that our azimuthal acceptance $\Delta\phi/2\pi$ is $\sim 1/45$ so that we should have few events with $\geq 2$ particles in the spectrometer acceptance.

Requested time.

Sufficient statistics for a given target at a given energy, together with target thickness and target-out studies, can be achieved in ~2 days. We propose to use 4 different targets and run at 3 different energies. In addition, we request 100 hours for initial set-up and debugging.

Time requested: 600 hours

Requested support.

We feel that our required support to set up and run this experiment makes minimal demands on NAL. We request:

1) trailer for electronics and personnel,

2) proper      type magnet with shielding plates,

3) assorted electronics from NAL equipment pool.

In particular,we note:

1) this experiment does not use a hydrogen target,

2) we do not require a large amount of floor space.

## References

1.  R. K. Adair, Phys. Rev. $\underline{D5}$, 1105 (1972).

2.  M. Jacob and R. Slansky, Phys. Letters 37B, 408 (1971).

3.  R. Hagedorn, Suppl. Nuovo Cimento $\underline{3}$, 147 (1965);
    R. Hagedorn and J. Ranft, ibid. $\underline{6}$, 169 (1968).

4.  J. Benecke, T. T. Chou, C. N. Yang, and E. Yen, Phys. Rev.
    $\underline{188}$, 2159 (1969); T. T. Chou and C. N. Yang, Phys. Rev.
    Letters $\underline{25}$, 1072 (1970).

5.  D. Amati, A. Stanghellini, and S. Fubini, Nuovo Cimento $\underline{26}$,
    896 (1962).

6.  F. Zachariasen and G. Zweig, Phys. Rev. $\underline{160}$, 1322 (1967);
    $\underline{160}$, 1326 (1967).

7.  R. P. Feynman, Phys. Rev. Letters $\underline{23}$, 1415 (1969); in $\underline{High}$
    $\underline{Energy\ Collisions}$, edited by C. N. Yang et al (Gordan $\underline{and}$
    $\underline{Breach;\ New\ York,}$ 1969).

8.  P. M. Fishbane and J. S. Trefil, preprint ITP-SB-73-10,
    Feb. 1973, Institute for Theoretical Physics, State University
    of New York at Stony Brook; P. M. Fishbane, J. S. Trefil and
    J. L. Newmeyer, preprint SLAC-PUB-1174, (TH) and (EXP),
    January 1973, Stanford Linear Accelerator Center.

9.  A. Dar and J. Vary, Phys. Rev. $\underline{D6}$, 2412 (1972).

10. G. Barry, preprint "Inclusive Reactions Involving Nuclei,"
    Purdue University.

11. Since each nucleon carries 1/A of the total c.m. momentum of
    the nucleus, the largest possible value for negative x is -1/A.

12. Belletini et al, NAL Conference (1972). This method is applicable
    only at ISR energies.

13. F. Sannes, W. E. Ellis, J. Norem, M. Silverman, and B. Maglic,
    Nuclear Inst, and Methods $\underline{92}$, 345 (1971).

14. W. R. Frazer, L. Ingber, C. H. Mehta, C. H. Poon, D. S. Silver-
    man, K. Stowe, P. D. Ting, H. J. Yesian, Rev. Mod. Phys. $\underline{44}$,
    284 (1972).

Summary of models, types of experiments, and the predictions made by various models.

| Experiment | (a) Mueller analysis | (b) Multiperipheral | (c) Diffractive fragmentation | (d) Statistical thermodynamical | (e) Cheng-Wu | Beam energy region |
|---|---|---|---|---|---|---|
| (1) Average multiplicity $\langle n(E) \rangle$ | $\langle n(E) \rangle = a \ln E + b$ | | No prediction; can accommodate any reasonable behavior | $\langle n \rangle$ grows faster than $\ln E$ | $\langle n \rangle \propto s^a, a>0$ | $E>E_p$ |
| (2) Multiplicity distribution $P(n)$ | No prediction | Roughly Poisson | $P(n) \propto n^{-1}$ if $\langle n \rangle \propto \ln E$ | No prediction | ? | $E>E_p$ |
| Partial cross sections $\sigma_n(E)$ | No prediction | $(K \ln s)^{n-2}s^{-K}/(n-2)!$, $K=2-2\alpha_M(0) \approx 1$ | Constant | No prediction | ? | $E>E_p$ |
| (3) One-particle spectra: limiting fragmentation? | Yes | Yes | Yes | Yes | No; $\rho(q) \propto s^a$ | $E>E_f$ |
| (4) One-particle spectra: central plateau? | Yes | Yes | No prediction; can be accommodated | Not in present version; can be accommodated | Yes | $E>E_p$ |
| (5) One-particle spectra: factorization in fragmentation regions | Yes | Yes | ? | No prediction | ? | $E>E_f$ |
| (6) One-particle spectra: factorization in plateau region | Yes | Yes | No | No prediction | ? | $E>E_p$ |
| (7) Two-particle spectra: correlations? | Only short-range correlations, if Regge poles $\gg$ Regge cuts. | | No prediction | No prediction | ? | $E>E_f$ |
| (8) Diffraction dissoc. into high missing mass | $\propto g_{PPP}^2$, triple Pomeron coupling | $g_{PPP}$ small or zero | "Favored" | No prediction | ? | |
| (9) $\sigma_{tot}(E)$ | $\sigma \propto$ const. or $s^{-\epsilon}$, $\epsilon \ll 1$. | | Constant | No prediction | $\sigma \propto \ln^2 s$ | |

TABLE 1   Ref. 14

( Table 2 is in text)

| Target | $\pi^+A \to \pi^+X$ | $\pi^+A \to \pi^-X$ | $pA \to \pi^+X$ | $pA \to \pi^-X$ |
|---|---|---|---|---|
| 1/2" carbon | 33.0 (570 000) | 7.0 (121 000) | 51.6 (890 000) | 20.0 (345 000) |
| 1/2" aluminum | 44.1 (762 000) | 9.4 (162 000) | 68.8 (1 189 000) | 26.7 (461 000) |
| 3/8" tin | 54.2 (936 000) | 11.5 (199 000) | 84.7 (1 464 000) | 32.9 (568 000) |
| 1/4" lead | 46.7 (807 000) | 12.2 (211 000) | 89.7 (1 550 000) | 34.8 (601 000) |

Table 3

Table 4

| x range | -(.1-.2) | -(.2-.3) | -(.3-.4) | -(.4-.5) | -(.5-.6) | -(.6-.7) | -(.7-.8) |
|---|---|---|---|---|---|---|---|
| $p_\perp$ range (MeV/c) | | | | | | | |
| 100-150 | 83 760 | 156 960 | 60 900 | 10 230 | 150 | - | - |
| 150-200 | 285 840 | 175 260 | 67 140 | 27 300 | 6 930 | 540 | - |
| 200-250 | 93 870 | 169 200 | 64 830 | 24 540 | 7 590 | 1 530 | 270 |
| 250-300 | 1 170 | 117 600 | 57 000 | 22 470 | 6 600 | 1 380 | 270 |
| 300-350 | - | 36 300 | 47 190 | 18 720 | 5 640 | 1 110 | 240 |
| 350-400 | - | 1 320 | 32 220 | 14 460 | 4 530 | 870 | 180 |
| 400-450 | - | - | 9 420 | 10 770 | 3 240 | 660 | 120 |
| 450-500 | - | - | 480 | 6 810 | 2 310 | 480 | 90 |
| 500-550 | - | - | - | 1 800 | 1 380 | 180 | - |
| Total | 464 640 | 656 640 | 339 180 | 137 100 | 38 370 | 6 750 | 1 170 |

Counts/day for p Al(1/2") $\rightarrow \pi^\pm$ X

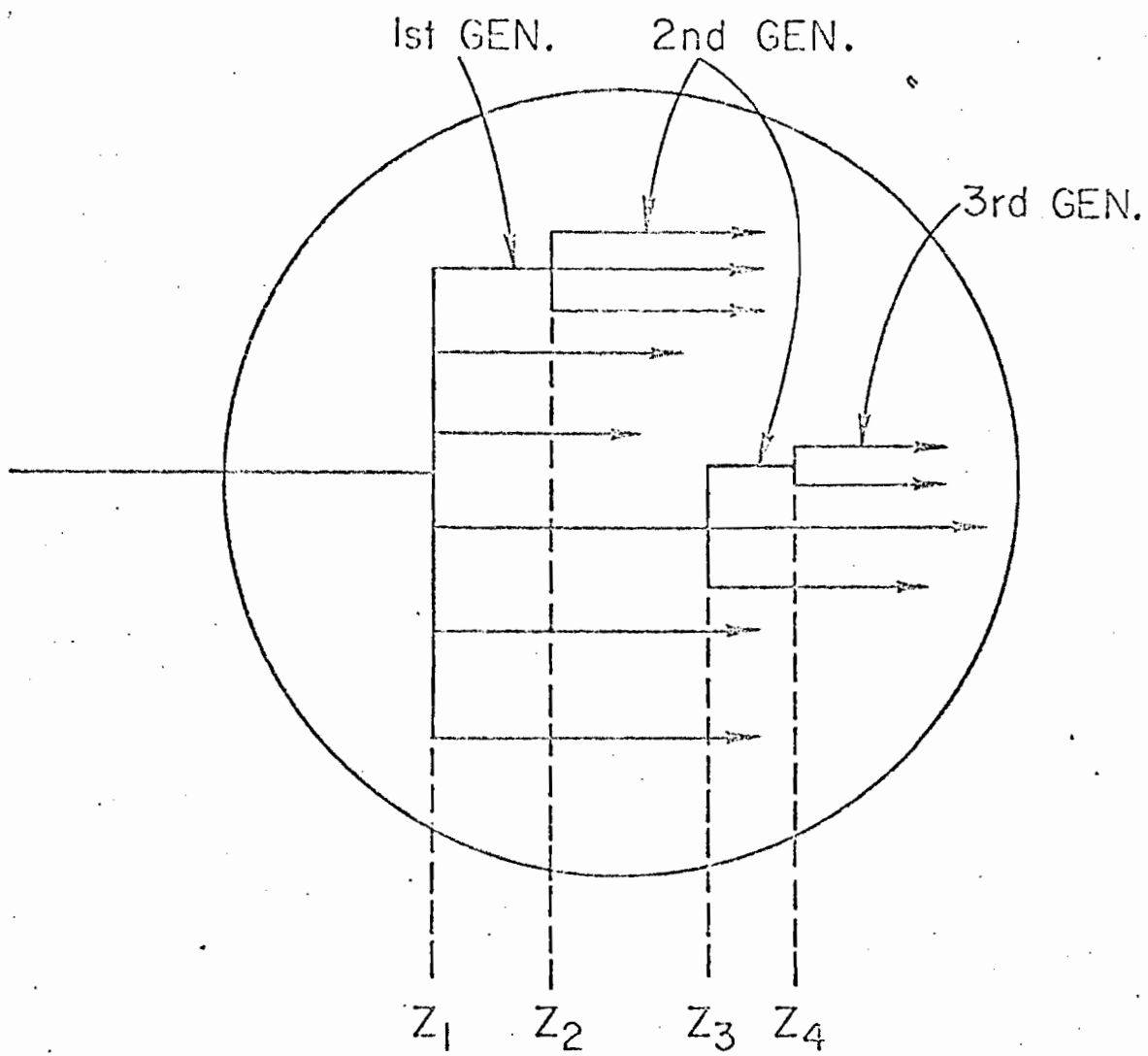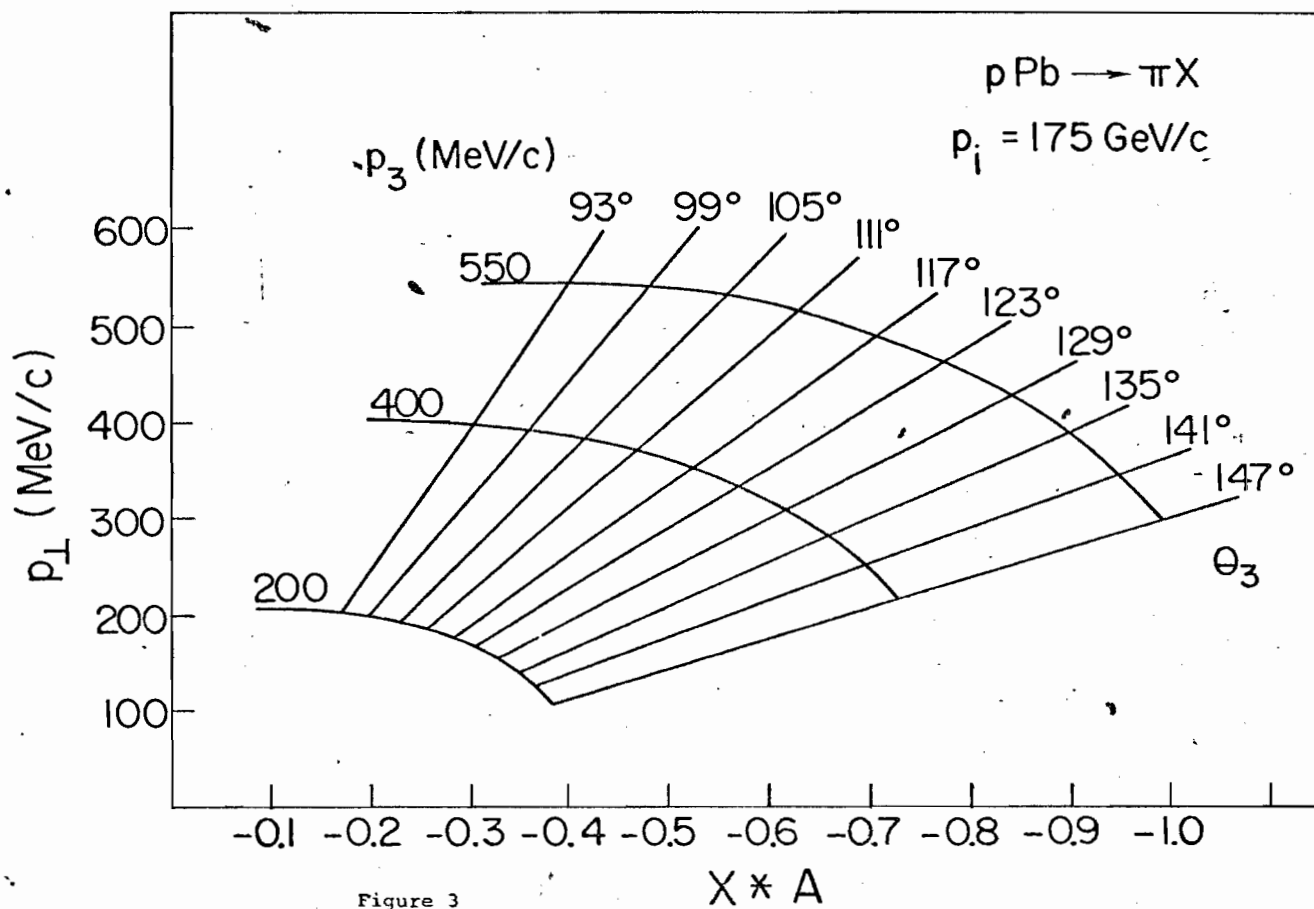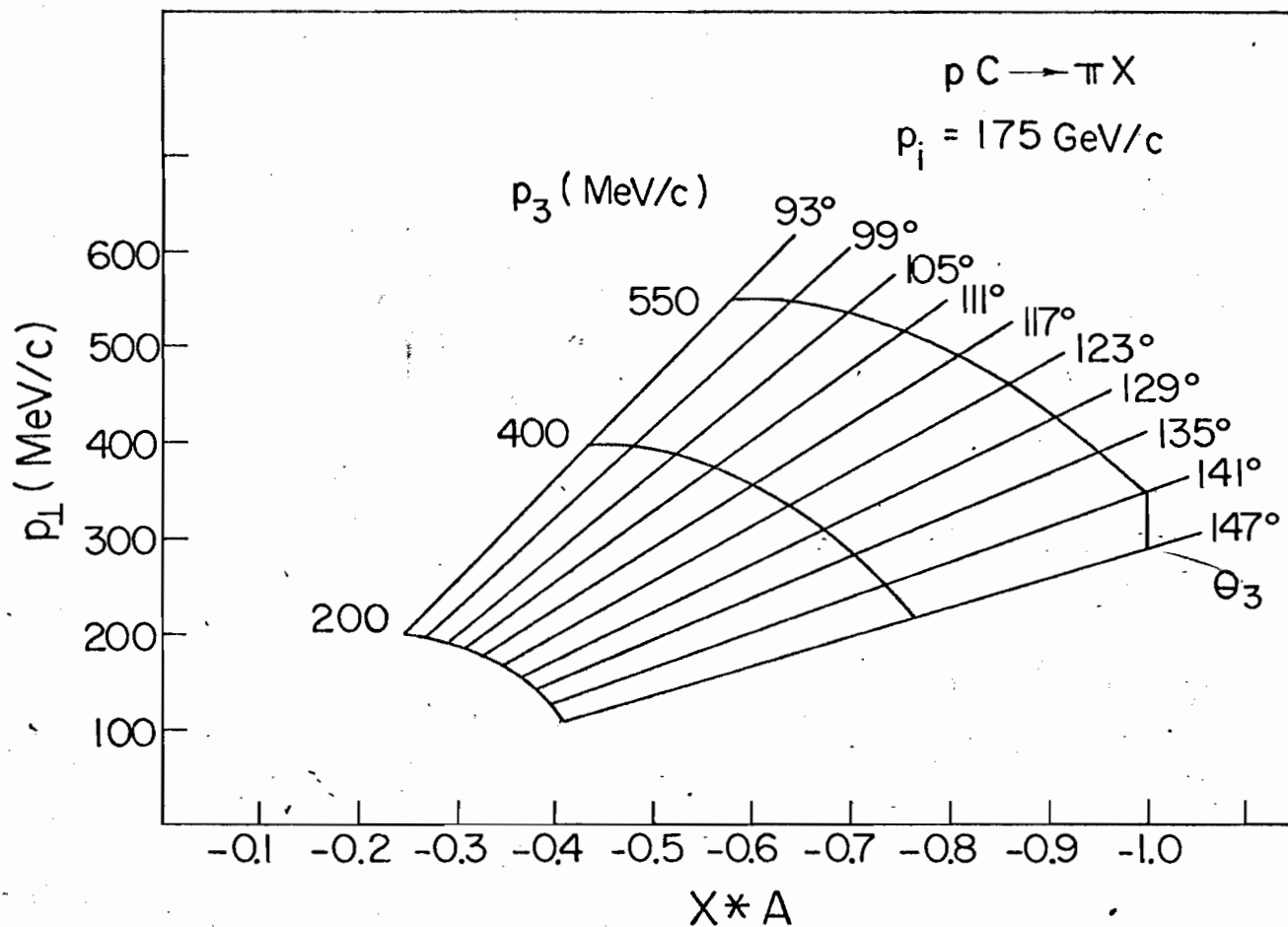Figure 1

Ist GEN.    2nd GEN.

3rd GEN.

$Z_1$    $Z_2$    $Z_3$    $Z_4$
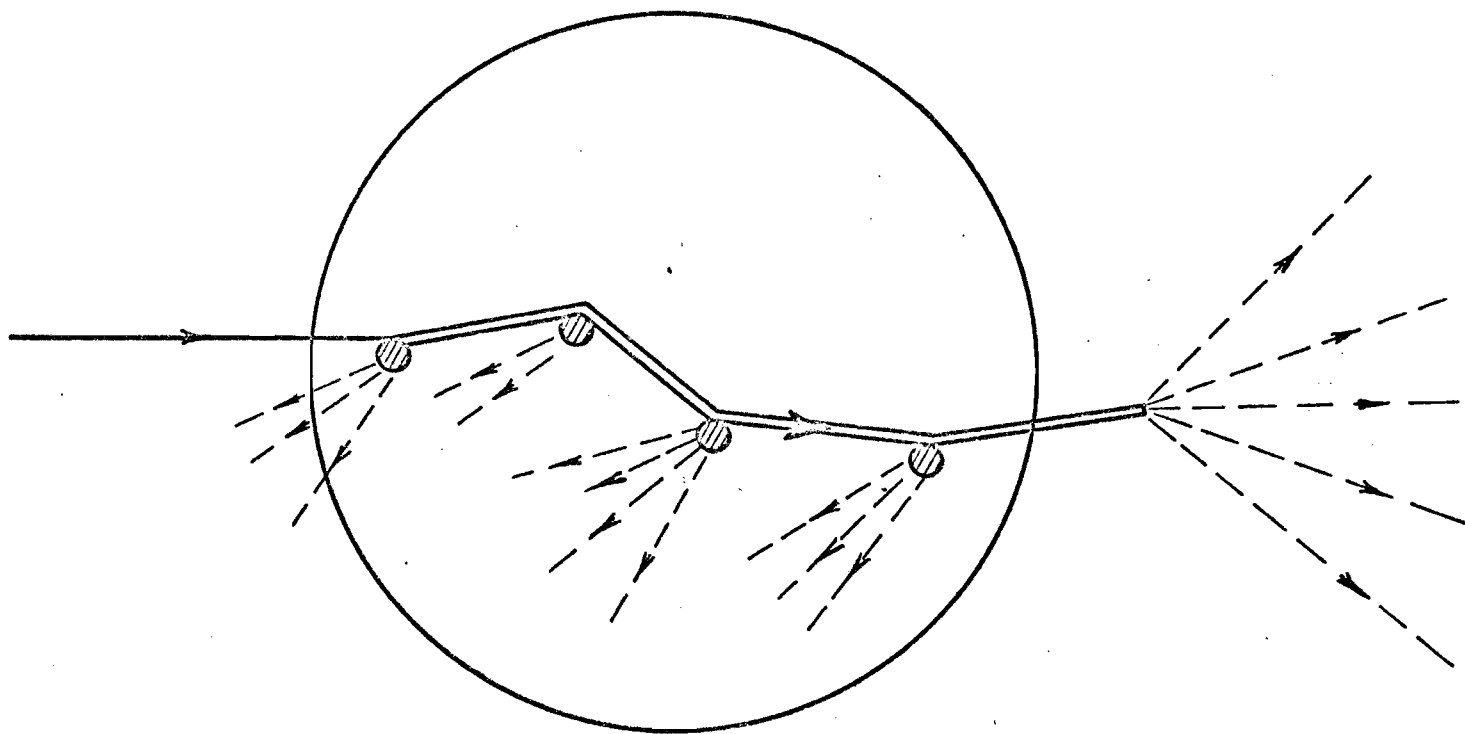
Fig. 2
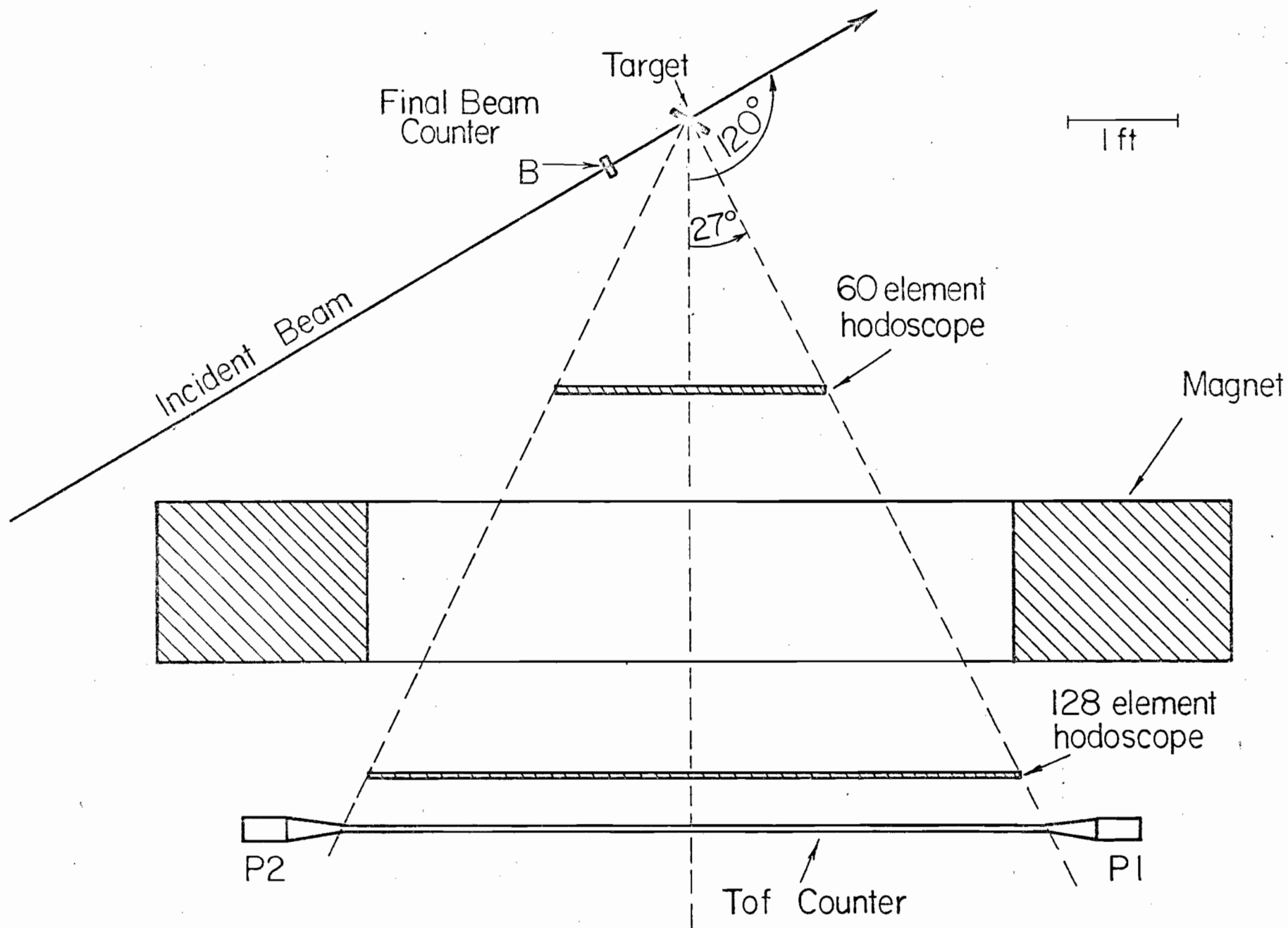
Figure 3

HODOSCOPE MAGNETIC SPECTROMETER

Figure 4

| | $P_3$ MeV/c | $\theta_3 - 120°$ rad |
|---|---|---|
| -1 | 200-300 | -0.40-(-0.30) |
| 2 | " | -0.05 - 0.05 |
| 3 | " | 0.30 - 0.40 |
| 4 | 350-450 | -0.40-(-0.30) |
| 5 | " | -0.05- 0.05 |
| 6 | " | 0.3 - 0.4 |

Resolution vs. Target Thickness for Aluminum

Resolution vs. Target Angle for Lead

Resolution vs. Target Thickness for Aluminum.

Resolution vs. Target Angle for Lead

$\Delta P_\perp$ (MeV/c)

$\Delta x$

t (inches)

$\phi$ (degrees)
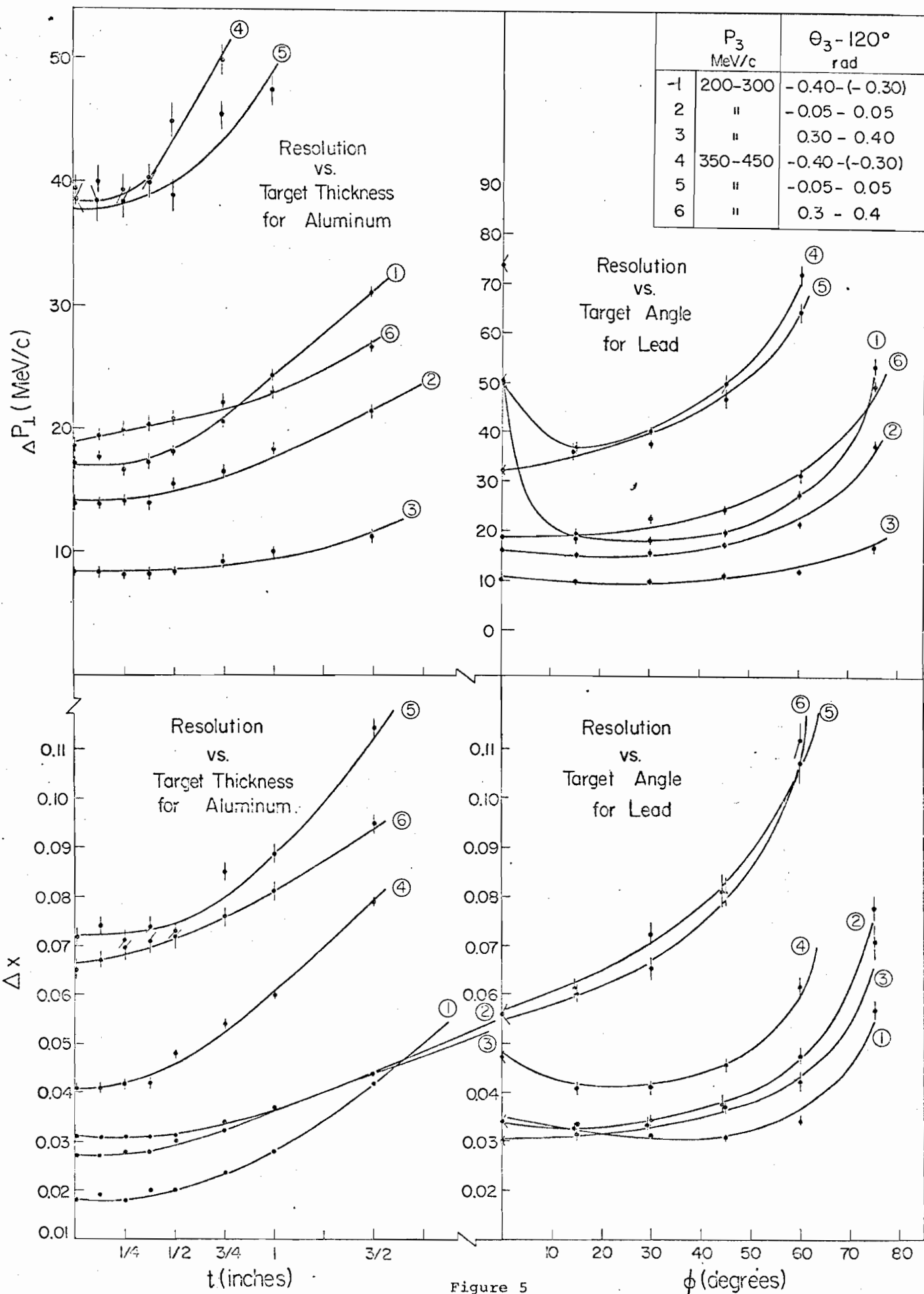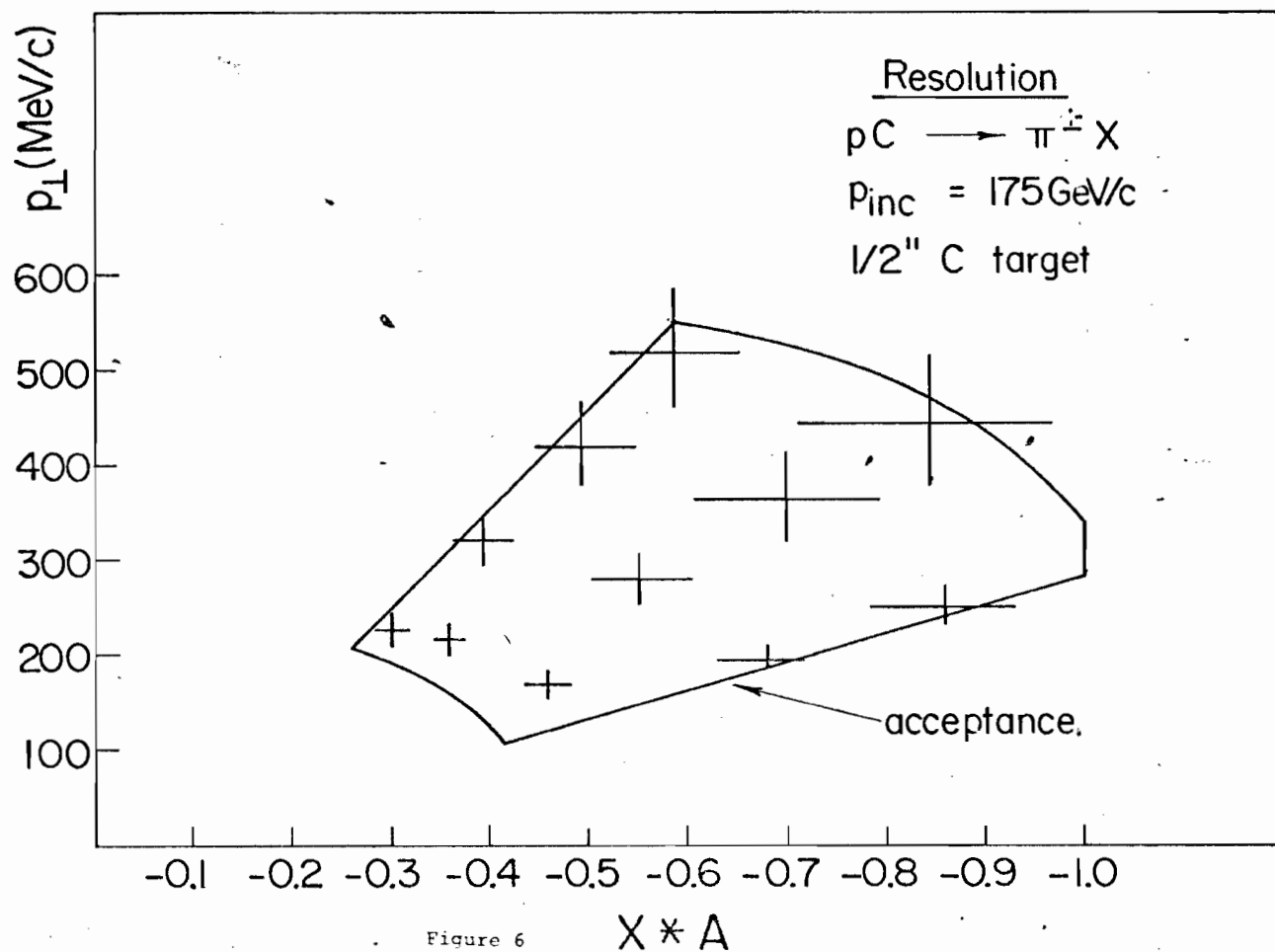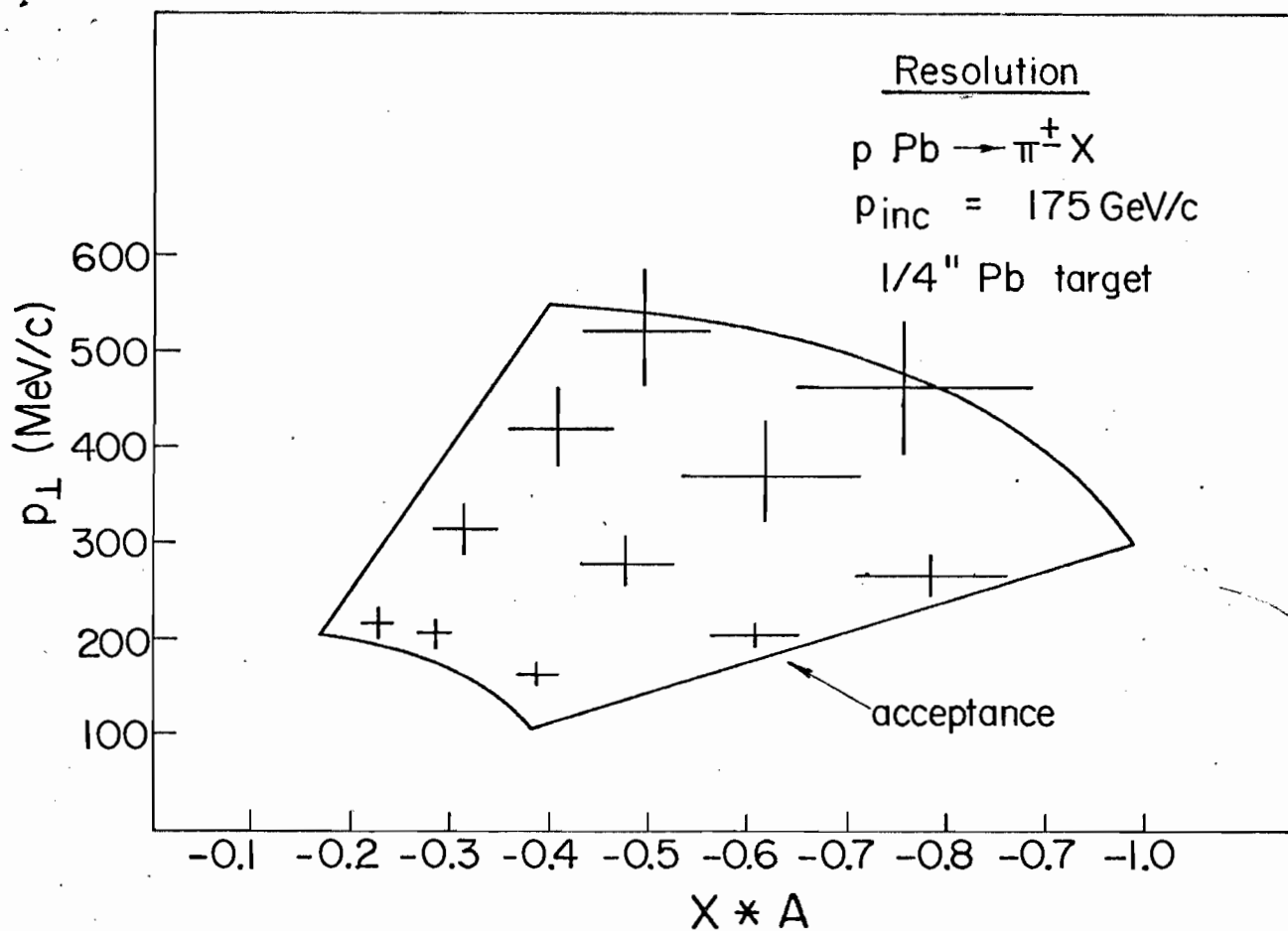
Figure 5

Figure 6

Addendum to NAL #210

**CORNELL UNIVERSITY**
LABORATORY OF NUCLEAR STUDIES
ITHACA, N. Y. 14850

May 21, 1973

Dr. Josh Alspector
Physics Department
Rutgers University
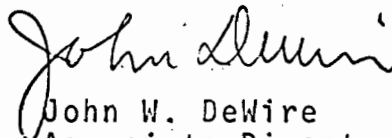New Brunswick, New Jersey 08903

Dear Dr. Alspector:

This is in response to your telephone call last week with regard to the availability of a wide aperture magnet for your use at NAL. The magnet we have is a PPA type 72D18, Mark II, for which I am enclosing an outline drawing which shows the principal dimensions. The magnet is equipped with a set of iron shields on either side of the gap to reduce the extent of the fringing field. The field has been carefully mapped by Dave Cassel, who also developed a set of programs for track reconstruction from a point target to a set of wire planes at the exit.

While we do not have a definite schedule for the magnet's use here, we would be reluctant to make a definite commitment to you until you have a well determined schedule for your use. We would be willing to make the magnet available to you for an eighteen month period starting at some future time when your plans are firm and there exists no need for us at that time. My guess is that we will be able to do this during the next year although something may come up to force us to change our plans.

We would expect you to be responsible for moving the magnet to NAL and returning it to us in good working condition. If your interest in the magnet goes beyond the proposed experiment, we would be happy to extend the loan for another year at any time, provided we do not have plans for it.

I suggest that you let us know when you have a definite schedule and we will give you a definite answer then.

Sincerely yours,

John DeWire

John W. DeWire
Associate Director
Laboratory of Nuclear Studies

JDW:mp
Enc.
cc: B.D. McDaniel
    H.E. Doney

Two experiments (#178 and #210) have been proposed at NAL to investigate production from complex nuclei. Although the primary motivations for these experiments are similar (to identify classes of models operative in multiparticle production), the measurements themselves are nearly orthogonal. To this extent, these proposals should be considered <u>complementary</u> rather than competitive. This is especially true in view of the model dependence of the predictions which have motivated these experiments.

A comparison of NAL #210 (Cohen <u>et al.</u>, Rutgers University) and NAL #178 (Busza <u>et al.</u>, MIT) is presented below.

<u>I.</u>
- Busza et al. propose to measure multiplicity distributions, $\sigma_n$

- Rutgers proposes to measure the inclusive cross section $\sigma_{inc}(p_\perp, x)$ as a function of $p_\perp$ and $x$, covering a large range in both variables and with good resolution. These two measurements are related by

$$\langle n \rangle = \frac{\sum n \, \sigma_n}{\sigma_{Tot}} = \frac{1}{\sigma_{Tot}} \int \frac{d\sigma_{inc}(p_\perp, x)}{dp_\perp \, dx} \, dp_\perp \, dx$$

Therefore, Rutgers can investigate:

a)  Does scaling from nuclei depend on the value of $x$, setting in first at larger x values?

b)  What is the $p_\perp$ dependence of $\sigma_{inc}$?

c)  Is $\sigma_{inc} = f(x)g(p_\perp)$ and what are these functions?

II.     - Busza et al. measure only the number of charged particles
        in each event
        - Rutgers distinguishes final state particles and charge,
        differentiating final state $\pi^+$, $\pi^-$, p, and $\bar{p}$.

        Therefore, Rutgers
            a) Determines the $\pi^+/\pi^-$ ratio
            b) Has no problems from $p, \bar{p}$ contamination.
            c) Determines inclusive cross sections for p and $\bar{p}$
               production together with the $\bar{p}/p$ ratio.

III.    - Busza et al. look mainly in the forward direction
        - Rutgers looks in the backward (target fragmentation)
        region with x<0.

        According to current models (e.g., Trefil and Fishbane)
        these regions are qualitatively quite different and can
        be expected to have different A dependences. The
        backward direction is probably more sensitive when
        investigating the A dependence of coherent (2-step)
        production since

$$\sigma_n = \underbrace{\int_0^1 \frac{d\sigma_n(x)}{dx} dx}_{\substack{\text{projectile} \\ \text{fragmentation} \\ \downarrow \\ \propto ( \text{?? (probably A} \\ \text{independent)}}} + \underbrace{\int_{-1}^0 \frac{d\sigma_n(x)}{dx} dx}_{\substack{\text{target} \\ \text{fragmentation} \\ \downarrow \\ A^{1/3} )}}$$

Therefore, in a measurement of $\sigma_n$ or $\sigma_{inc}$, the forward part
can wash out the A dependence in coherent production processes.

IV.     Current models for inclusive production from complex

nuclei currently analytically integrate over $p_\perp$ in their

predictions of the energy and A dependence. Since both

#178 and #210 experimentally have a low momentum cutoff

on final state charged particles it may be necessary to

correct for this in analysis. This will require a knowledge

of the $p_\perp$ dependence of $\sigma_{inc}$. Rutgers will experimentally

determine this function while Busza et al. will experimen-

tally integrate $p_\perp$ from the cutoff value to $p_\perp = \infty$.

## III. Two Component Model of Multiparticle Production

Recently many authors have investigated a two component theory of multiparticle production by analyzing multiplicity distributions produced in hadron collisions[1,2,3]. We assume that two classes of production mechanisms can contribute to inclusive cross sections:

i) coherent production processes (fireball,etc.) - $\sigma_{coh}$

ii) incoherent production processes (multiperipheral,etc.) - $\sigma_{inc}$

So the measured inclusive cross section is

$$\sigma_{inc} = P_{coh} \sigma_{coh} + P_{incoh} \sigma_{incoh}$$

where $P_{coh}$ and $P_{incoh} = 1 - P_{coh}$ are the relative probabilities for coherent and incoherent production respectively. In general, $P_{coh}$ and $P_{incoh}$ can be energy dependent.

$\sigma_{coh}$ and $\sigma_{incoh}$ will have different A dependences for production from complex nuclei. In the backward direction (target fragmentation region) we expect:

$$\sigma_{coh} \propto A^{1/3} \sigma_{inel} \propto A \quad \text{or} \quad \sigma_{coh} = \sigma_{inc}(hp) A$$

and

$$\sigma_{incoh} \propto (\text{A-independent} \xrightarrow[s \to \infty]{} A) \quad \sigma_{inel} \propto A^{2/3} \xrightarrow[s \to \infty]{} A^{5/3}$$

or,

$$\sigma_{incoh} = \sigma_{inc}(hp) A^{n(s)}$$

where $2/3 \leq n(s) \leq 5/3$ is a function of the total c.m. energy squared, s, and $\sigma_{inc}(hp)$ is the inclusive hadron-proton cross section. Thus,

$$\sigma_{inc} = P_{coh} \sigma_{inc}(hp) A + (1 - P_{coh}) \sigma_{inc}(hp) A^{n(s)}$$

or $\quad \sigma_{inc}/A = P_{coh} \sigma_{inc}(hp) + (1 - P_{coh}) \sigma_{inc}(hp) A^{n(s)-1}$.

If, $p_{coh} = 1$ then $\sigma_{inc}/A$ should show no A dependence. Otherwise, at each energy we can fit our data with the above form and extract $p_{coh}$ and $n(s)$ at each energy.

References:

1.  H. Harari and E. Rabinovici, Physics Letters 43B (1973) 49.

2.  K. Fiałkowski and H.I. Miettinen, Phys. Lett. 43B (1973) 61.

3.  L. Van Hove Physics Letters 43B (1973) 65.

## IV.  COMMENT ON REQUESTED TIME FOR NAL #210.

NAL proposal #210 requests 600 hours to investigate 4 elements (C, Al, Sn, Pb) at 3 energies ( $p_{inc}$ = 50, 100, and 200 GeV/c). If this amount of time is felt to be excessive in view of other NAL commitments, a more modest effort could investigate 2 energies and 3 elements. This would cut the data taking in half without having a serious effect on the experiment. With this option the requested time would be 350 hours.